

Grain size dependence of surface plasmon enhanced photoluminescence

Xiaoying Xu,^{1,*} Mitsuru Funato,² Yoichi Kawakami,² Koichi Okamoto,^{1,3,4} and Kaoru Tamada¹

¹Institute for Advanced Chemistry and Materials, Kyushu University, 6-10-1 Hakozaki, Higashi-ku, Fukuoka 812-8581, Japan

²Department of Electronic Science and Engineering, Kyoto University, Katsura Campus, Nishikyo-ku, Kyoto 615-8510, Japan

³PRESTO, Japan Science and Technology Agency, 4-1-8 Honcho Kawaguchi, Saitama 332-0012, Japan

⁴okamoto@ms.ifoc.kyushu-u.ac.jp

*xux1@ms.ifoc.kyushu-u.ac.jp

Abstract: Photoluminescence (PL) in the InGaN quantum well based light-emitting diodes (LED) is greatly mediated through the coupling with the Surface Plasmons (SPs) at the interface of the sputtered Ag film. SPs coupled PL is independently tuned through controlling the grain size of the sputtered Ag films. The grain size of ~50 nm exhibits the maximum light extraction efficiency (LEE) at the wavelength of 460 nm. This grain size agrees with the periodic lattice constant of the grating structure in the calculation, where the momentum mismatch between the SPs and the radiative light can be compensated.

©2012 Optical Society of America

OCIS codes: (240.6680) Surface plasmons; (250.5230) Photoluminescence; (240.0310) Thin films; (240.5770) Roughness.

References and links

1. K. Okamoto, I. Niki, A. Shvartsner, Y. Narukawa, T. Mukai, and A. Scherer, "Surface-plasmon-enhanced light emitters based on InGaN quantum wells," *Nat. Mater.* **3**(9), 601–605 (2004).
2. J. Henson, E. Dimakis, J. DiMaria, R. Li, S. Minissale, L. Dal Negro, T. D. Moustakas, and R. Paiella, "Enhanced near-green light emission from InGaN quantum wells by use of tunable plasmonic resonances in silver nanoparticle arrays," *Opt. Express* **18**(20), 21322–21329 (2010).
3. K. Okamoto, I. Niki, A. Scherer, Y. Narukawa, T. Mukai, and Y. Kawakami, "Surface Plasmon enhanced spontaneous emission rate of InGaN/GaN quantum wells probed by time-resolved photoluminescence spectroscopy," *Appl. Phys. Lett.* **87**(7), 071102 (2005).
4. T. S. Oh, H. Jeong, Y. S. Lee, J. D. Kim, T. H. Seo, H. Kim, A. H. Park, K. J. Lee, and E. K. Suh, "Coupling of InGaN/GaN multi-quantum-wells photoluminescence to surface plasmons in platinum nanocluster," *Appl. Phys. Lett.* **95**(11), 111112 (2009).
5. M. K. Kwon, J. Y. Kim, B. H. Kim, I. K. Park, C. Y. Cho, C. C. Byeon, and S. J. Park, "Surface-plasmon-enhanced light-emitting diodes," *Adv. Mater. (Deerfield Beach Fla.)* **20**(7), 1253–1257 (2008).
6. A. Neogi, C.-W. Lee, H. O. Everitt, T. Kuroda, A. Tackeuchi, and E. Yablonovitch, "Enhancement of spontaneous recombination rate in a quantum well by resonant surface plasmon coupling," *Phys. Rev. B* **66**(15), 153305 (2002).
7. W. L. Barnes, "Light-emitting devices: turning the tables on surface plasmons," *Nat. Mater.* **3**(9), 588–589 (2004).
8. C. H. Lu, C. C. Lan, Y. L. Lai, Y. L. Li, and C. P. Liu, "Enhancement of green emission from InGaN/GaN multiple quantum wells via coupling to surface plasmons in a two dimensional silver array," *Adv. Funct. Mater.* **21**(24), 4719–4723 (2011).
9. L.-W. Jang, T. Sahoo, D.-W. Jeon, M. Kim, J.-W. Jeon, D.-S. Jo, M.-K. Kim, Y.-T. Yu, A. Y. Polyakov, and I.-H. Lee, "Quantum efficiency control of InGaN/GaN multi-quantum-well structures using Ag/SiO₂ core-shell nanoparticles," *Appl. Phys. Lett.* **99**(25), 251114 (2011).
10. C. Y. Cho, K. S. Kim, S. J. Lee, M. K. Kwon, H. D. Ko, S. T. Kim, G. Y. Jung, and S. J. Park, "Surface plasmon-enhanced light-emitting diodes with silver nanoparticles and SiO₂ nano-disks embedded in p-GaN," *Appl. Phys. Lett.* **99**(4), 041107 (2011).
11. L.-W. Jang, D.-W. Jeon, T. Sahoo, D.-S. Jo, J.-W. Ju, S.-J. Lee, J.-H. Baek, J.-K. Yang, J.-H. Song, A. Y. Polyakov, and I.-H. Lee, "Localized surface Plasmon enhanced quantum efficiency of InGaN/GaN quantum wells by Ag/SiO₂ nanoparticles," *Opt. Express* **20**(3), 2116–2123 (2012).

12. L.-W. Jang, J.-W. Ju, D.-W. Jeon, J.-W. Park, A. Y. Polyakov, S.-J. Lee, J.-H. Baek, S.-M. Lee, Y.-H. Cho, and I.-H. Lee, "Enhanced light output of InGaN/GaN blue light emitting diodes with Ag nano-particles embedded in nano-needle layer," *Opt. Express* **20**(6), 6036–6041 (2012).
13. C. Hums, T. Finger, T. Hempel, J. Christen, A. Dadgar, A. Hoffmann, and A. Krost, "Fabry-Perot effects in InGaN/GaN heterostructures on Si-substrate," *J. Appl. Phys.* **101**(3), 033113 (2007).
14. M. Jamshidnejad, I. Kazeminejad, and A. Razeghizadeh, "Simulation of silver thin films' growth and influence of deposition rate on final grain size under angle flux and standard situation," *Int. Nano Lett.* **1**(1), 59–61 (2011).
15. Z. Rakocevic, R. Petrovic, and S. Strbac, "Surface roughness of ultra-thin silver films sputter deposited on a glass," *J. Microsc.* **232**(3), 595–600 (2008).
16. J. M. Delgado, J. M. Orts, and A. Rodes, "A comparison between chemical and sputtering methods for preparing thin-film silver electrodes for in situ ATR-SEIRAS studies," *Electrochim. Acta* **52**(14), 4605–4613 (2007).
17. K. Okamoto and Y. Kawakami, "High-Efficiency InGaN/GaN Light Emitters Based on Nanophotonics and Plasmonics," *IEEE J. Sel. Top. Quantum Electron.* **15**(4), 1199–1209 (2009).
18. P. B. Johnson and R. W. Christy, "Optical constants of the noble metals," *Phys. Rev. B* **6**(12), 4370–4379 (1972).
19. D. Edward, Palik, *Handbook of Optical Constants of Solids* (Academic Press, Boston, 1985).

1. Introduction

InGaN quantum well (QW) based light-emitting diodes (LEDs) with high emitting efficiency has been developed due to the coupling with the Surface Plasmons (SPs). A 14-fold enhancement of photoluminescence (PL) has been observed in the system of single InGaN QW coated with the thermal-evaporated Ag film [1]. The coupling between the SPs at the interface of the metal film and photon-excited excitons in the QW is crucial to achieve the enhancement, when the resonance energy of the SPs ($h\omega_{sp}$) and that of the excitons are close. And hence, the energy in the excitons can be transferred to that of SPs. The external quantum efficiency of LED (η_{ext}) is given by a product of the internal quantum efficiency (IQE; η_{int}) and the light extraction efficiency (LEE; C_{ext}) [1,2]. The SPs provide a higher density of states and a faster spontaneous emitting rate, which will lead to the enhancement of the IQE [3–6]. The SPs can later be converted to radiate light by introducing a grating structure to compensate the wave vector mismatch between the SPs and the emitting light [7,8], which will otherwise dissipate into heat. This determines the LEE. Therefore, a higher enhancement ratio can be achieved by increasing both the IQE and the LEE.

Several papers have been reported to increase the IQE by tuning the SP energy to meet that of the excitons. A proper metal, for example Ag, can be chosen to have the closest Surface Plasmon Polariton (SPP) energy to that of the excitons [1,3]. Localized Surface Plasmon (LSP) can also couple with the excitons [4,5,9–12]. The size, shape of the metallic nanoparticle [4,5], and the capping SiO₂ layer [9,10] will also affect the coupling strength between the LSP and the exciton, and thus the IQE. However, in this SP-coupled QW LEDs, the coupling between the SPs and the photons, *i.e.* the LEE is lack of systematic study. A hole-array structure in the p-GaN layer [8] and an ordered grating structure [1] have been employed to increase the LEE. The film roughness can also play an important role in the LEE [1]. However, till now, how the film roughness will have influence on the SP enhanced LEE is still an open question.

In this paper, we investigate the PL enhancement ratio as a function of the grain size in the Ag films deposited on top of the InGaN QW LEDs by magnetron sputtering method at various growth rates. We find out that an optimized grain size is required to enhance the PL.

2. Experimental methods

The schematic illustration of the sample structure is shown in Fig. 1(a). The InGaN/GaN QW layers were grown on the Sapphire (0001) substrate by metal-organic chemical vapor deposition (MOCVD). A three micron thick GaN layer was first deposited on the two-side polished Sapphire substrate, which was followed by three alternate InGaN/GaN layers (3 and 10 nm thick respectively). Afterwards, a 50 nm thick Ag film was grown on top of GaN spacer layer by magnetron sputtering deposition (Sanyu Electron, SVC-700RF). The thickness of the Ag films was monitored by the mass microbalance. The growth rates of the

Ag films were controlled by changing the applied plasma energy. The deposition pressure was kept constant at 0.43 Pa. As a result, the grain size of the Ag film varied in a range from 38 to 140 nm. The PL spectra, excited by an InGaN diode laser (Edmond Industrial Optics) at the wavelength of 405 nm, were collected from the back side of the wafer (Sapphire side) by use of a multichannel spectrometer (Ocean Optics USB2000). All the samples were half covered by a shadow mask during the Ag deposition. Therefore, we can directly compare the PL microscopy images as well as the PL spectra of the samples with and without the metal film. The uncertainty from the composition inhomogeneity in the QW can be excluded since all the measurements were carried out on the same sample. All the PL spectra shown in the paper are normalized by taking the PL peak intensity of uncoated InGaN QW at 460 nm as unity 1.

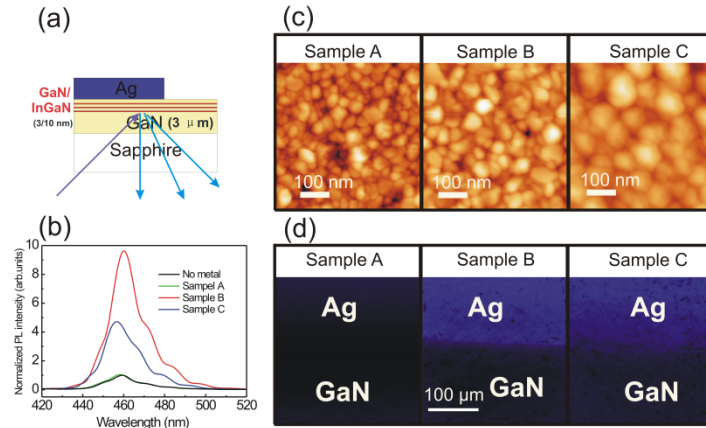


Fig. 1. (a) The schematic illustration of the sample structure. The laser (405 nm) is incident from the Sapphire side and photoluminescence is collected from the same side. (b) Normalized PL intensity vs. the wavelength for Sample A, B, C and QW without Ag film. All the PL spectra shown in the paper are normalized by taking the PL peak intensity of uncoated InGaN QW at 460 nm as unity 1. Sample A, B and C were grown at different deposition rates, 2.9, 1.0 and 0.4 Å/S, respectively. AFM and PL microscopy images are shown in (c) and (d) for sample A, B and C.

3. Results and discussion

Figure 1(b) shows the normalized PL spectra of three typical samples, sample A, B and C. The Ag films of these three samples were deposited at different growth rates, 2.9, 1.0 and 0.4 Å/S respectively. The corresponding AFM images (500×500 nm) are presented in Fig. 1(c). The grain size of the Ag film increases when the growth rate decreases. The average grain sizes of sample A, B and C are 38, 50 and 87 nm respectively. The intensity of the PL varies with the grain size of the Ag film, shown in Fig. 1(b). Sample B, with a moderate growth rate 1.0 Å/s, possesses the most efficient enhancement ratio, ~ 9.3 -fold at the peak position of the PL spectra. Both sample A and C have the lower PL peak intensity values compared with sample B. Sample C has an enhancement ratio around 4.5-fold, while sample A has almost no enhancement at the peak position. The emission wavelength at the peak position varies ($\sim \pm 3$ nm) at different spots on the wafer due to the inhomogeneity of the Indium composition in the InGaN layer. The Fabry-Pérot oscillation introduced by the high refractive index of GaN will have little effect on the PL enhancement [13] considering the different reflectivity of the two interfaces, Air/GaN and Ag/GaN for without and with Ag coated samples. PL microscopy images for these three samples are shown in Fig. 1(d). All the images were taken under the same condition. The PL enhancement by coupling with SPs is straightforward in the images. Sample A has almost no enhancement and sample B exhibits the highest enhancement. The enhancement of sample C is in between. It is clear that the grain size of the Ag film does have

influence on the PL intensity in this system. The grain size of about 50 nm offers the maximum enhancement ratio.

Next, we investigate systematically the evolution of the grain size of the Ag film with different growth rates in Fig. 2(a). The growth rates were controlled by changing the Ar⁺ plasma energy during the Ag deposition. The grain size decreases exponentially with the growth rate in Fig. 2(a). The similar behavior of grain size dependence on the growth rate has been reported theoretically [14] and experimentally [15,16] by the other groups in the Ag film system. In Fig. 2(a), the experimental data can be fitted using the following equation: $p = p_0 \times e^{(-r/r_0)} + p_1$. $p_0 = 148$ nm, $p_1 = 40$ nm and $r_0 = 0.39$ Å/S. p is the grain size in the Ag film. r is the growth rate of the Ag film. r_0 is proportional to the horizontal diffusion rate of the Ag atoms on the surface of the film plane. A high r_0 value indicates that a larger grain size is preferred in the Ag film. p_0 is determined by the roughness in the GaN spacer layer. Since the horizontal diffusion rate is high for Ag, a minimum grain size of 40 nm is observed in our experiment. The standard deviation values calculated from the statistical distribution of the grain size in the Ag films have been plotted as the error bars in Fig. 2(a). The statistical distribution of the grain size in sample C is shown as the inset figure, with the standard deviation about 20 nm. The statistical distribution of the grain size does not vary much from sample to sample at different growth rates in Fig. 2(a). Figure 2(b) shows the PL enhancement at the peak position (460 nm) as a function of the grain size of the Ag film. The PL enhancement has a peak value (~10.1-fold) at the average grain size of ~50 nm. Either larger or smaller grain size will not enhance more. The IQE has been reported in our previous works to be 6% in the InGaN QW without metal coating, which has increased to 40% after Ag coating from the temperature dependence PL measurements [1,17]. After excluding the enhancement effect of the non-resonant light scattering (Fabry-Pérot effect included), the IQE of sample B is expected to be enhanced 4.0 times with Ag coating at the peak position. The Full-Width Half-Maximum (FWHM) of the curve plotted in Fig. 2(b) is about 35 nm. From Fig. 2(b), we conclude that a specific grain size has to be chosen to optimize the PL enhancement.

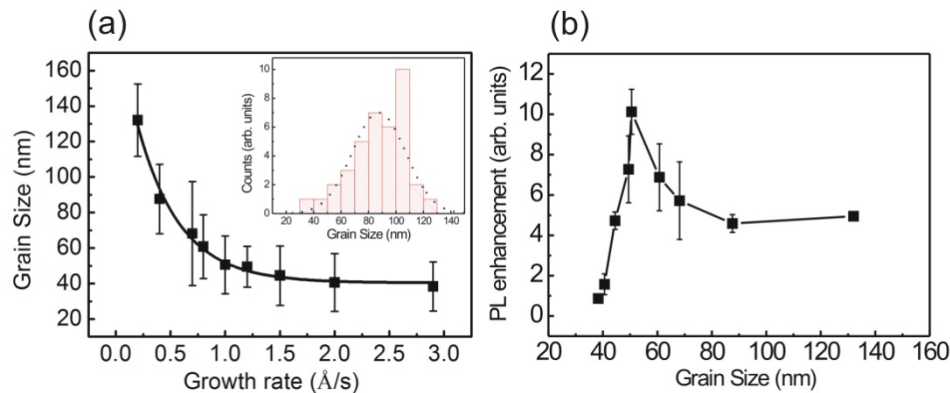


Fig. 2. (a) Grain size of the Ag film vs. growth rate. The inset figure presents the statistical distribution of the grain size in the Ag film in sample C. The dotted line is the guide to the eye. (b) PL enhancement vs. the grain size of the Ag film.

In order to understand the physics behind the experimental result shown in Fig. 2(b), we made a theoretical calculation based on SPP. The contribution from the LSP is neglected for the following reasons: (1) The roughness of the Ag film is less than 10 nm, which is far below the film thickness of 50 nm. The Ag film does not form isolated islands but a continuous film. (2) According to the Fröhlich condition ($2\epsilon_{Ag} + \epsilon_{GaN} = 0$), the LSP resonance wavelength is at 531 nm when one Ag nanoparticle with the size smaller than the light wavelength is

embedded in the GaN wafer, which will be hard to couple with the blue QW LED. The external quantum efficiency of the light emission (η_{ext}) is determined by the IQE and the LEE. And the IQE is mainly determined by the non-radiative (k_{non}) and the radiative (k_{rad}) recombination rate of the excitons which are excited by the incident light. The equation follows as:

$$\eta_{ext} = C_{ext} \times \eta_{int} = C_{ext} \times \frac{k_{rad}}{k_{rad} + k_{non}}$$

The spontaneous emission rate is becoming faster with the coupling to the SPs, for that the exciton-SP coupling rate are much faster than the recombination rates of excitons. The enhanced spontaneous emission rate by SPs is given by the Fermi's golden rule and depends mainly on the density of states of the SPP [3,6]. Here in our experiments, all the samples are 50 nm in thickness. The resonance energy and the density of states of the SPs are presumed to be the same. Therefore, the enhanced spontaneous emission rate by SPs is presumed to be the same for all the samples, hence the IQE also should be the same. Since the grain size changes among the samples, we believe that only the LEE changes accordingly, which therefore, determines the variation of the PL enhancement. Since the SPs have the larger momentum than the light, only by losing the momentum, the energy of the SPs can be extracted as the radiative light. The wave vector mismatch between SPs and light can be compensated by adding a grating structure. Light will be emitted once the reciprocal lattice vectors fit the following equations, shown in the inset of Fig. 3.

$$k_{sp} - k_l = G_{ij} = \frac{2\pi}{a_{max}}, k_{sp} + k_l = G_{ij} = \frac{2\pi}{a_{min}}. \quad (1)$$

k_{sp} , k_l are the wave vectors of the SP and the light. Only the first order reciprocal lattice vector G_{10} or G_{01} is considered in the above equations. The higher order G_{ij} is ignored because it is relatively smaller than G_{10} and G_{01} . Since all the light with the momentum inside the light cone can be extracted, a range of reciprocal lattice vectors can fulfill the requirements of momentum compensation. Then, periodic lattice constant a of the grating structure, with a range between a_{min} and a_{max} will meet the requirements to extract the light. k_{sp} and k_l can be obtained by the following equations:

$$k_{sp}(\omega) = \frac{\omega}{c} \sqrt{\frac{\epsilon'_{Ag}(\omega)\epsilon_{GaN}(\omega)}{\epsilon'_{Ag}(\omega) + \epsilon_{GaN}(\omega)}}, k_l(\omega) = \frac{\omega}{c} \sqrt{\epsilon_{GaN}(\omega)}. \quad (2)$$

ϵ'_{Ag} and ϵ_{GaN} are the real parts of dielectric constants of Ag and GaN, respectively. Combining Eq. (1) and (2), the maximum and minimum periodic lattice constants of the grating are obtained.

$$a_{max}(\lambda) = \frac{\lambda}{\sqrt{\frac{\epsilon'_{Ag}(\lambda)\epsilon_{GaN}(\lambda)}{\epsilon'_{Ag}(\lambda) + \epsilon_{GaN}(\lambda)} - \sqrt{\epsilon_{GaN}(\lambda)}}} \quad (3)$$

$$a_{min}(\lambda) = \frac{\lambda}{\sqrt{\frac{\epsilon'_{Ag}(\lambda)\epsilon_{GaN}(\lambda)}{\epsilon'_{Ag}(\lambda) + \epsilon_{GaN}(\lambda)} + \sqrt{\epsilon_{GaN}(\lambda)}}}$$

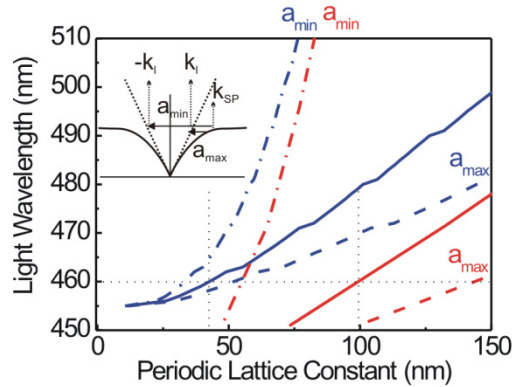


Fig. 3. Extracted light wavelength as a function of the periodic lattice constant of the Ag film. The dashed and dash-dotted lines are the boundary curves (maximum and minimum periodic lattice constants) to extract the light at the specific wavelength. The solid lines are the average values. Red and blue curves are derived from two sets of dielectric constants of Ag, Johnson and Christy and Palik, respectively. The horizontal dotted line presents the emission wavelength at 460 nm. The vertical dotted lines denote the optimal grain size to emit the wavelength at 460 nm for dielectric constants of Ag using Palik (left) and Johnson and Christy (right) data. The inset illustrates the wave vector mismatch between the Surface Plasmons and the light.

We present the calculation curves of the correlation between the periodic lattice constant and the PL extraction wavelength based on the SPP model in Fig. 3. Two sets of curves are drawn in the figure with the use of two sets of dielectric constant values of Ag, the red one from Johnson and Christy [18] and the blue one from Palik data sheets [19]. The dashed and dash-dotted lines illustrate two boundary curves of the maximum and minimum periodic lattice constants to be able to extract the light. And the solid lines are the average periodic lattice constant. The range of the periodic lattice constants 101.5 ± 45.7 nm and 42.6 ± 9.4 nm can be used to emit the light at the wavelength of 460 nm for different Ag dielectric constants, Johnson and Christy and Palik, respectively. In the experiment, the grain is considered to work as a random grating structure. Then the grain size should agree with the periodic lattice constant obtained from the calculation. Therefore, from theoretical calculation, a peak in the curve of the PL enhancement vs. the grain size is expected in the experiment. We did observe a peak at the grain size of 50 nm with FWHM equaling to 35 nm in Fig. 2(b). The experimental result is consistent with the calculation using the Palik's data, which has a peak at 42.6 nm. The randomness of the grain size limited by the current growth method, may broaden FWHM in the experiment. The asymmetric peak shape in Fig. 2(b) is also consistent with the calculation result. In Fig. 3, the slopes of the two boundary lines are different. At the wavelength of 460 nm, the slope of the a_{\min} line is more than that of the a_{\max} line. Therefore, a small change of the periodic lattice constant at the a_{\min} side will cause the SPs to uncouple into the radiation mode. On the contrary, at the a_{\max} side, it is still possible to extract the light even the periodic lattice constant changes quite a few. In the experiment, a sharper slope is also observed at the small grain size side. In Fig. 2(b), the Ag film with the grain size of 40 nm (10 nm smaller than grain size at the peak) shows almost no enhancement, while that with the grain size of 60 nm (10 nm larger) still has a high enhancement ratio, about 6.9-fold. The discrepancy between the experimental observations and the calculation on the large grain side might be attributed to the coupling between the SPs and the emission light via the high order reciprocal lattice vector matching, which has been ignored in our calculation. The experimental results agree with the calculation in these two aspects. (1) The optimized grain size of 50 nm agrees with the average periodic constant 42.6 nm calculated with the Palik dielectric constants for Ag to extract the light at the wavelength of 460 nm. (2) The

asymmetric peak in the curve of PL enhancement vs. grain size is attributed to the different slopes in the boundary in the calculation. Therefore, the grains in the Ag film are of crucial importance in the process of light extraction, which are considered to work as the random grating structure.

4. Conclusion

In conclusion, we observe a maximum value of the PL enhancement in the InGaN/GaN QW based LED which couples with the SPs at the interface of the sputtered 50 nm thick Ag films with the grain size of ~50 nm. The grain size of the Ag film, controlled through sputtering deposition rate, plays an important role in the PL enhancement, especially in the LEE. IQE is assumed to be constant since all the Ag films have the same thickness of 50 nm. According to the calculation, the light at a specific wavelength can be extracted from the SPs with the periodic lattice constants of the Ag grating structure in a limited range. The grains in the Ag film work as a random grating structure in the experiment. An appropriate grain size of the Ag film needs to be selected before the experiment in order to enhance the PL most efficiently. Our finding leads to the potential of maximizing the Surface-Plasmon enhanced photoluminescence through optimizing the metallic film structure with the use of a low cost physical vapor deposition method.

Acknowledgments

This work was supported by the Precursory Research for Embryonic Science and Technology (PRESTO) at Japan Science and Technology Agency (JST).